

Defining Trigonometric Box Spline On Type-I Triangulation

Hrushikesh Jena ^{*}and Mahendra Kumar Jena [†]

Abstract

In this paper, trigonometric box spline surface is defined using a subdivision scheme. The subdivision scheme is derived using the non-stationary subdivision scheme that has been defined in (Jena et. al., A non-stationary subdivision scheme for generalizing trigonometric spline surfaces to arbitrary meshes, *Computer Aided Geom. Design*, 20, (2003), 61-77). A convergence analysis is also given. It is found that the limit surface of the proposed non-stationary subdivision scheme does not satisfy the convex hull property, while $\cos^2 h$ times the limit surface satisfy the convex hull property where h is the mesh size with $0 < h < \frac{\pi}{3}$.

2010 AMS Subject Classification: 65D07, 65D17.

Keywords: Arbitrary Topology, Subdivision algorithm, Trigonometric spline.

1 Introduction

Subdivision schemes [5, 6, 7, 8] are the schemes which are used to generate parametric curves and surfaces from a finite set of control points in $R^d (d \geq 1)$, iteratively. Initially, a control polygon or a

^{*}Department of Mathematics, Veer Surendra Sai University of Technology, Burla, Odisha 768018, India, email: jehrushikesh@gmail.com

[†]Department of Mathematics, Veer Surendra Sai University of Technology, Burla, Odisha 768018, India, email: maheny2010@gmail.com

control mesh is given. From this a new refined polygon or mesh is generated by applying a subdivision algorithm once. So, by repeated application of the subdivision algorithm, a sequence of control polygons or control meshes are obtained. In the limit, the sequence of control polygons or control meshes converge to a smooth curve or surface for a suitably chosen subdivision rule. A subdivision scheme is called a stationary subdivision scheme, if the subdivision rule is same at all levels of iteration. Otherwise it is called a non-stationary subdivision scheme.

The idea of generating smooth free form surfaces from arbitrary topology by iterated mesh refinement started in 1978 when two papers [2] and [4] appeared back to back in the same issue of Computer Aided Design. The Doo-Sabin and Catmull-Clark algorithm represent generalizations of the subdivision schemes for bi-quadratic and bi-cubic B-splines, respectively.

Standard CAD geometries are usually represented in terms of tensor product B-splines and their rational version NURBS[19, 21]. Tensor product representation is computationally very efficient but unable to model with complicated shapes and also in doing local mesh refinements. On the otherhand, splines over triangulations overcome such disadvantages. Box splines are an attractive alternative which combine several advantages from tensor product B-splines and splines over triangulations[1, 11]. One of the most important advantages of box splines is that they can handle more complex domains than the corresponding tensor product counterparts.

Trigonometric spline curves play an important role in shape designing and geometric modeling. They were first introduced by Schoenberg [20]. The recurrence relations and the divided differences for them were studied by Lyche and Winther [12]. Trigonometric splines can be expressed by several ways. One way to express is by linear combination of trigonometric B-splines. Another way to study trigonometric splines is by non-stationary subdivision algorithm[7]. They are very useful since they are used to draw circles and other conics. Like polynomial splines, they can also be generalized to multivariate setting. Koch[9] introduced multivariate trigonometric B-splines which are found suitable for CAGD.

Besides these very few literatures are available in this area. For example, a non-stationary subdivision algorithm for the evaluation of trigonometric spline curves with uniform knots [7] and its generalization to a trigonometric version of the Doo-Sabin algorithm for generating surfaces from meshes of arbitrary topology[8].

Comparing to other mesh, triangular meshes are much more flexible to be adapted to arbitrary topology. Furthermore, trigonometric box splines defined over type-I triangular partitions provide certain flexibility comparing to tensor product splines as described earlier. So the main goal of our study is to define trigonometric box spline surface using a non-stationary subdivision scheme over type-I triangulation.

The main motivation for our work comes from the paper of Jena et.al.[8], where tensor product bi-quadratic spline surfaces are constructed over arbitrary topology. It is a non-stationary subdivision scheme and produces extraordinary vertices for type I triangulation. In our present work, after applying the subdivision algorithm as defined in [8] to an initial control mesh of type-I triangulation, we apply another averaging scheme to it. However in contrast to [8], after each iteration of this new scheme we always get a regular type-I triangular mesh. Thus, we get a limit surface which is free of any extraordinary points. Since box splines are free of extraordinary points, this justifies our nomenclature. Also, we have shown that our new subdivision scheme converges and the limit surface is uniformly continuous. Moreover, after normalization the limit surface satisfies the convex hull property.

The paper is structured as follows. In Section 2, we briefly review the nonstationary scheme defined in [8]. Next, in Section 3, we introduce our new nonstationary subdivision scheme which generates trigonometric box spline surfaces on an initial mesh of type-I triangulation. In Section 4, we give the convergence of our proposed subdivision scheme. Here, it is emphasized that the convergence of our subdivision scheme is of same order as that of [8]. Finally, we give a conclusion in Section 5.

2 Trigonometric Spline Surface on Arbitrary Topology

In this section, we briefly review the construction of trigonometric spline surface on arbitrary topology.

First, we present the subdivision scheme[8] for an arbitrary topology. Let \mathcal{F}^0 be the initial control mesh.

Let F_0 be a face of \mathcal{F}^0 with ordered vertices A_1, A_2, \dots, A_n . A set of new vertices associated with the face F_0 and the old vertices A_i s are obtained by the following subdivision rule.

Subdivision Rule (R_1):

$$a_i = \frac{P + E_i + E_{i-1} + F}{4}, \quad i = 1, 2, \dots, n \quad (2.1)$$

where

$$P = \frac{A_i}{\cos^2(h/2)}, \quad E_i = \frac{A_i + A_{i+1}}{2\cos^2(h/2)\cosh},$$

and

$$F = \frac{1}{\cos^2(h)\cos^2(h/2)} \frac{A_1 + \dots + A_n}{n},$$

where all the indices are taken modulo n . Here, h is the mesh size which also controls the shape of the surface and $0 < h < \frac{\pi}{3}$. After simplification it is obtained that

$$a_i = \alpha(n, 1)A_i + \beta(n, 1)A_{i-1} + \beta(n, 1)A_{i+1} + \gamma(n, 1)(A_{i+2} + \dots A_{i+n-2}), \quad (2.2)$$

where for $k \geq 1$,

$$\gamma(n, k) = \frac{1}{4n} \frac{1}{\cos^2(h/2^k)\cos^2(h/2^{k-1})},$$

$$\beta(n, k) = \gamma(n, k) + \frac{1}{8\cos^2(h/2^k)\cos(h/2^{k-1})},$$

and

$$\alpha(n, k) = \gamma(n, k) + \frac{1}{4\cos^2(h/2^k)\cos(h/2^{k-1})} + \frac{1}{4\cos^2(h/2^k)}.$$

Applying the connectivity rule of Doo-Sabin scheme[4] to the new vertices associated with all the faces of \mathcal{F}^0 , a new control mesh \mathcal{F}^1 is generated. The whole subdivision process is denoted by an operator \mathcal{S}_1 , i.e., $\mathcal{F}^1 = \mathcal{S}_1\mathcal{F}^0$. Repeating this process, \mathcal{F}^2 is generated from \mathcal{F}^1 using the subdivision rule

R_2 . In general, the k^{th} control mesh \mathcal{F}^k is generated from \mathcal{F}^{k-1} using the subdivision rule R_k , where in the subdivision rule R_k ($k > 1$); $\alpha(n, 1)$, $\beta(n, 1)$ and $\gamma(n, 1)$ are replaced by $\alpha(n, k)$, $\beta(n, k)$ and $\gamma(n, k)$, respectively. The values $\alpha(n, k)$, $\beta(n, k)$ and $\gamma(n, k)$ are called mask associated with the rule R_k . The subdivision process is expressed by

$$\mathcal{F}^k = \mathcal{S}_k \mathcal{F}^{k-1} = \mathcal{S}_k \mathcal{S}_{k-1} \dots \mathcal{S}_1 \mathcal{F}^0 = \mathcal{S}^{(k)} \mathcal{F}^0. \quad (2.3)$$

The connectivity rule used in [8] produces a new face of valence n from an old face of valence n ; a new face of valence n from an old interior vertex of valence n and new quadrilateral from an old interior edge. Therefore, after each iteration number of quadrilaterals increases where the number of non-quadrilaterals remains unchanged. After each iteration the face sizes also decrease. However, the interior non-quadrilateral faces become surrounded by layers of quadrilaterals. As a result, the layers of quadrilaterals converge to a tensor product bi-quadratic spline and the non-quadrilateral faces shrink to extraordinary points.

3 Trigonometric Box Spline

In this section, we construct a new subdivision scheme that generates surfaces from the control points lying on a mesh of a type-I triangulation. Let X_0 be such a control mesh which has six triangular faces joined as shown in Figure 1(Left). Applying the subdivision scheme as discussed in the previous section to one of the triangular faces of X_0 , we get three new points(intermediate points). Since the faces are triangular we take $n = 3$. For example, the face $\{P_1, P_2, P_3\}$ gives new intermediate points q_1, q_7 and q_8 near the vertices P_1, P_2 and P_3 respectively. Similarly, other triangular faces also generate three new points each. In total, we get 18 new control points (q_1 to q_{18}) which are indexed as shown in the Figure 1(Right). Out of the eighteen points, six intermediate points q_1 to q_6 are associated with the central vertex point P_1 , which is also a vertex of each triangular face of X_0 . In particular, after applying the subdivision scheme as described in previous section, we get

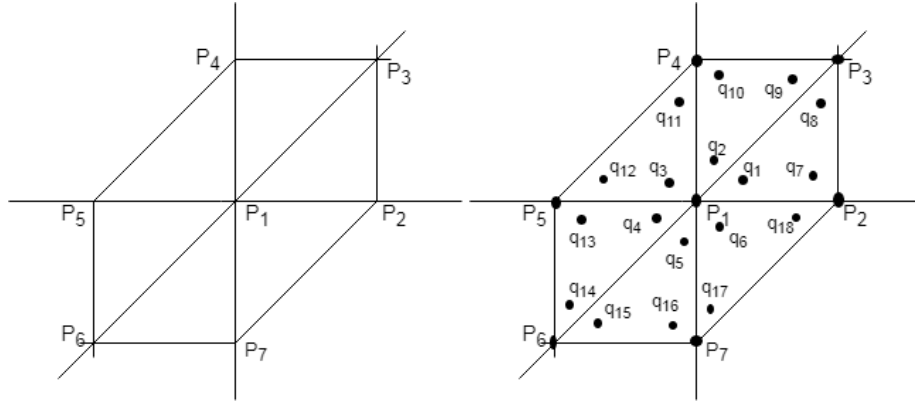


Figure 1: (Left)Initial Control mesh X_0 , (Right)Control mesh X_0 alongwith 18 intermediate points q_1 to q_{18} .

$$q_i = \alpha(3, 1)P_1 + \beta(3, 1)(P_{i+1} + P_{i+2}), \quad i = 1, 2, \dots, 6, \quad (P_8 = P_2).$$

The other points q_7 to q_{18} are computed as follows:

$$\begin{aligned} q_7 &= \alpha(3, 1)P_2 + \beta(3, 1)(P_3 + P_1), & q_8 &= \alpha(3, 1)P_3 + \beta(3, 1)(P_1 + P_2), \\ q_9 &= \alpha(3, 1)P_3 + \beta(3, 1)(P_4 + P_1), & q_{10} &= \alpha(3, 1)P_4 + \beta(3, 1)(P_1 + P_3), \\ q_{11} &= \alpha(3, 1)P_4 + \beta(3, 1)(P_5 + P_1), & q_{12} &= \alpha(3, 1)P_5 + \beta(3, 1)(P_1 + P_4), \\ q_{13} &= \alpha(3, 1)P_5 + \beta(3, 1)(P_6 + P_1), & q_{14} &= \alpha(3, 1)P_6 + \beta(3, 1)(P_1 + P_5), \\ q_{15} &= \alpha(3, 1)P_6 + \beta(3, 1)(P_7 + P_1), & q_{16} &= \alpha(3, 1)P_7 + \beta(3, 1)(P_1 + P_6), \\ q_{17} &= \alpha(3, 1)P_7 + \beta(3, 1)(P_2 + P_1), & q_{18} &= \alpha(3, 1)P_2 + \beta(3, 1)(P_1 + P_7). \end{aligned}$$

where,

$$\begin{aligned} \gamma(3, 1) &= \frac{1}{12\cos^2(h/2)\cos^2(h)}, \\ \beta(3, 1) &= \gamma(3, 1) + \frac{1}{8\cos^2(h/2)\cos(h)} = \frac{2 + 3\cosh}{24\cos^2(h/2)\cos^2(h)}, \\ \alpha(3, 1) &= \gamma(3, 1) + \frac{1}{4\cos^2(h/2)\cos(h)} + \frac{1}{4\cos^2(h/2)} = \frac{1 + 3\cosh + 3\cos^2(h)}{12\cos^2(h/2)\cos^2(h)}. \end{aligned}$$

Now, we describe our new subdivision scheme. In this scheme, we obtain the first level control points

Q_1 to Q_7 as follows:

$$Q_1 = \frac{1}{6} \sum_{i=1}^6 q_i = a_1 P_1 + a_2 (P_2 + \dots + P_7),$$

$$Q_2 = \frac{\frac{1}{2}(q_1 + q_6) + \frac{1}{2}(q_7 + q_{18})}{2} = b_1 (P_1 + P_2) + b_2 (P_7 + P_3).$$

In similar fashion, other points are obtained as

$$Q_3 = b_1 (P_1 + P_3) + b_2 (P_2 + P_4), Q_4 = b_1 (P_1 + P_4) + b_2 (P_3 + P_5),$$

$$Q_5 = b_1 (P_1 + P_5) + b_2 (P_4 + P_6), Q_6 = b_1 (P_1 + P_6) + b_2 (P_5 + P_7),$$

$$Q_7 = b_1 (P_1 + P_7) + b_2 (P_6 + P_2),$$

where, the weights are $a_1 = \frac{6(1+3\cosh+3\cos^2(h))}{72\cos^2(h/2)\cos^2(h)}$, $a_2 = \frac{2+3\cosh}{72\cos^2(h/2)\cos^2(h)}$,

$b_1 = \frac{4+9\cosh+6\cos^2 h}{48\cos^2(h/2)\cos^2(h)}$ and $b_2 = \frac{2+3\cosh}{48\cos^2(h/2)\cos^2(h)}$.

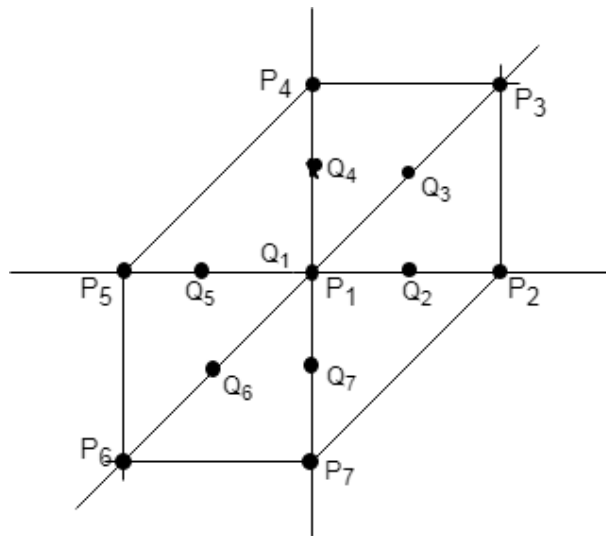


Figure 2: Old control points P_1 to P_7 and new control points Q_1 to Q_7 .

We categorize new control points as vertex points and edge points. The vertex points are those points which correspond to an old vertex point(valence 6), for example Q_1 . Similarly, edge points are those

points which correspond to an edge, for example Q_2 to Q_7 . A triangular face of a control mesh contains a vertex point and two edge points (See Figure 2).

Connectivity Rule : In a triangular face:

- (i) Join vertex points to edge points.
- (ii) Join edge points to edge points.

After this connectivity rule, we get a new control mesh. Below, we present our subdivision algorithm in a traditional way.

Subdivision Algorithm:

$$\begin{aligned} p_{2i,2j}^{k+1} &= w_0(k)p_{i,j}^k + w_1(k)(p_{i+1,j}^k + p_{i+1,j+1}^k + p_{i,j+1}^k + p_{i-1,j}^k + p_{i-1,j-1}^k + p_{i,j-1}^k), \\ p_{2i+1,2j}^{k+1} &= w_2(k)(p_{i,j}^k + p_{i+1,j}^k) + w_3(k)(p_{i+1,j+1}^k + p_{i,j-1}^k), \\ p_{2i+1,2j+1}^{k+1} &= w_2(k)(p_{i,j}^k + p_{i+1,j+1}^k) + w_3(k)(p_{i+1,j}^k + p_{i,j+1}^k), \\ p_{2i,2j+1}^{k+1} &= w_2(k)(p_{i,j}^k + p_{i,j+1}^k) + w_3(k)(p_{i+1,j+1}^k + p_{i-1,j}^k). \end{aligned}$$

Here $w_0(k)$, $w_1(k)$, $w_2(k)$ and $w_3(k)$ are the weights a_1 , a_2 , b_1 and b_2 , respectively in which h is replaced by $\frac{h}{2^k}$ (See Figure 3). Moreover, $p_{i,j}^k; (i, j) \in \mathbb{Z}^2, k = 0, 1, 2, \dots$ are the k -th level control points.

Applying this subdivision algorithm and then the connectivity rule iteratively, we get a limit surface.

Let X_k be the control mesh at k -th level and X_{k+1} be the control mesh at the $(k+1)$ -th level. X_{k+1} is obtained from X_k . In matrix form this subdivision scheme is written as

$$X_{k+1} = M_{k+1}X_k, \quad k = 0, 1, 2, \dots,$$

where,

$$\begin{aligned} X_k &= [p_{i,j}^k, p_{i+1,j}^k, p_{i+1,j+1}^k, p_{i,j+1}^k, p_{i-1,j}^k, p_{i-1,j-1}^k, p_{i,j-1}^k]^T, \\ X_{k+1} &= [p_{2i,2j}^{k+1}, p_{2i+1,2j}^{k+1}, p_{2i+1,2j+1}^{k+1}, p_{2i,2j+1}^{k+1}, p_{2i-1,2j}^{k+1}, p_{2i-1,2j-1}^{k+1}, p_{2i,2j-1}^{k+1}]^T, \end{aligned}$$

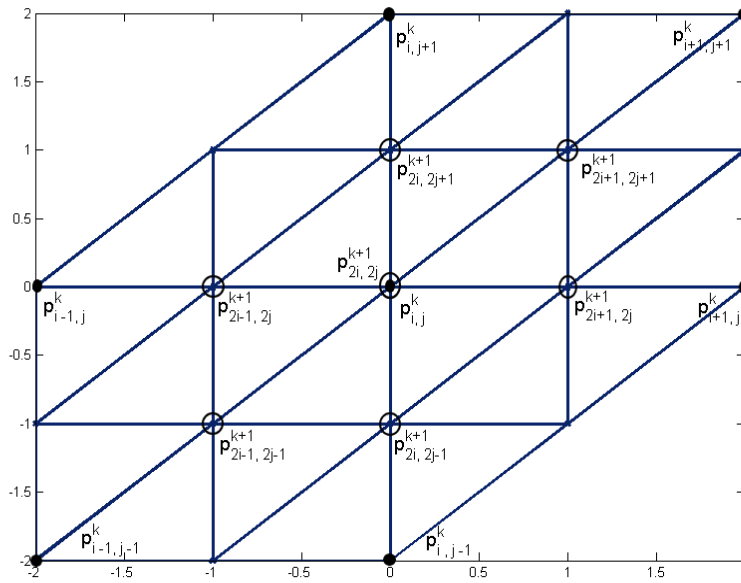


Figure 3: k -th level (points represented by black dot) control mesh X_k and $(k + 1)$ -th level (points represented by non-filled circles) control mesh X_{k+1} .

and M_{k+1} is the $(k + 1)$ -th level subdivision matrix which is given by

$$M_{k+1} = \begin{bmatrix} w_0(k) & w_1(k) & w_1(k) & w_1(k) & w_1(k) & w_1(k) & w_1(k) \\ w_2(k) & w_2(k) & w_3(k) & 0 & 0 & 0 & w_3(k) \\ w_2(k) & w_3(k) & w_2(k) & w_3(k) & 0 & 0 & 0 \\ w_2(k) & 0 & w_3(k) & w_2(k) & w_3(k) & 0 & 0 \\ w_2(k) & 0 & 0 & w_3(k) & w_2(k) & w_3(k) & 0 \\ w_2(k) & 0 & 0 & 0 & w_3(k) & w_2(k) & w_3(k) \\ w_2(k) & w_3(k) & 0 & 0 & 0 & w_3(k) & w_2(k) \end{bmatrix}_{7 \times 7} \quad (3.1)$$

Trigonometric Box Spline : Let the initial control mesh Y_0 be given by the Figure 4 in which $p_{0,0}^0 = 1$ and rest control points have values 0. We apply the subdivision scheme (subdivision algorithm + connectivity rule) to Y_0 a number of times to get a limit surface. For example, applying the subdivision scheme 3 times to the initial control mesh Y_0 in Figure 4, we get a limit surface Y_3 as shown in Figure 5. This limit surface is called as the trigonometric box spline. We observe that this spline surface does not lie in the convex hull of initial control mesh Y_0 . Note that, the sum of all entries of each row of

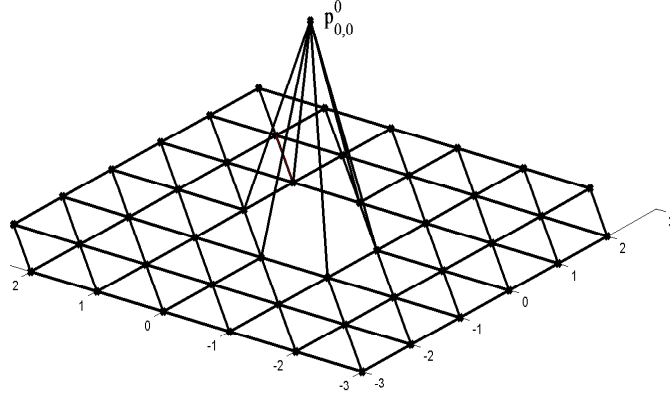


Figure 4: Initial control mesh Y_0 showing $p_{0,0}^0 = 1$.

subdivision matrix M_{k+1} is $\frac{\cos^2(\frac{h}{2^{k+1}})}{\cos^2(\frac{h}{2^k})}$. Again, we have

$$\frac{\cos^2 \frac{h}{2} \cdot \cos^2 \frac{h}{4} \cdots \cos^2(\frac{h}{2^{k+1}})}{\cos^2 h \cdot \cos^2 \frac{h}{2} \cdots \cos^2(\frac{h}{2^k})} = \frac{\cos^2(\frac{h}{2^{k+1}})}{\cos^2 h},$$

which tends to $\frac{1}{\cos^2 h}$ as k approaches to ∞ . So $\cos^2 h$ times the limit surface lies in the convex hull of initial control mesh of Y_0 . To show this we multiply $\cos^2 h$ to k -th level control mesh (See Figure 6). Thus, we call $\cos^2 h$ times the limit surface as the normalized trigonometric box spline.

4 Convergence Analysis

In this section, we present the convergence analysis of our non-stationary subdivision scheme. In our scheme

$$Y_{k+1} = M_{k+1} Y_k,$$

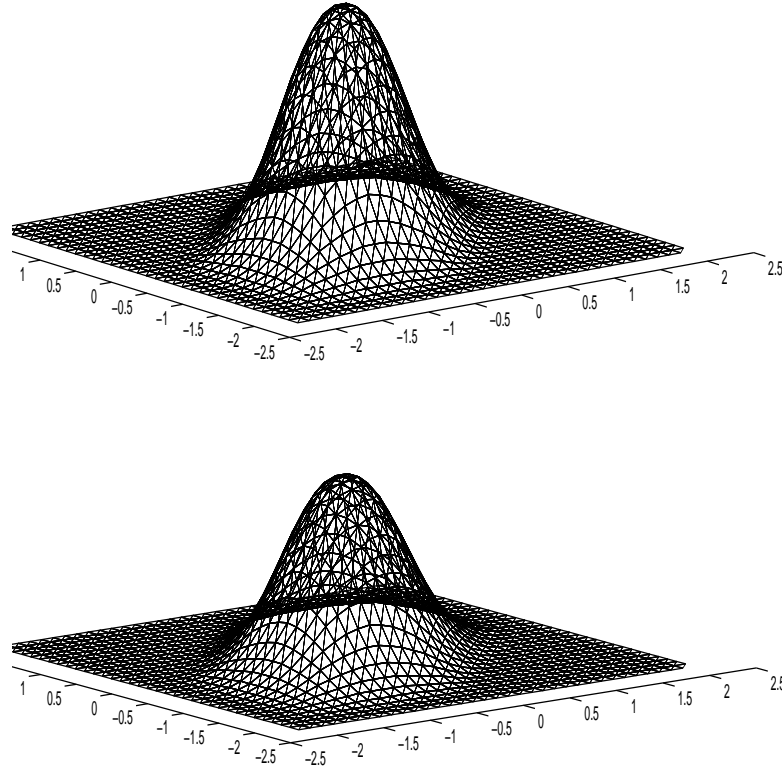


Figure 5: Non-normalized (top) and Normalized (bottom) Trigonometric Box Spline. Limit surface is taken after three iterations (Y_3). Here we have taken $h = 1$.

where M_{k+1} is a 7×7 matrix termed as $(k + 1)$ -th level subdivision matrix. From this, we get

$$\begin{aligned} Y_{k+1} &= M_{k+1}Y_k = M_{k+1}M_kY_{k-1} \\ &= M_{k+1}M_k \dots M_1Y_0 =: M^{(k+1)}Y_0. \end{aligned}$$

For the study of the convergence, we need the stationary matrix M , which is obtained from M_k by putting $h = 0$. Let $S_{k+1} := M_{k+1} - M$. It is observed that entries of the matrix M_{k+1} are non-negative and non-increasing with k . The sum of all the entries in each row of M_k is $\frac{\cos^2(h/2^k)}{\cos^2(h/2^{k-1})}$, and each entry of M_k is greater than the corresponding entry of M . Overall, our matrix M_k behaves identically with that of M_k in [8]. Therefore, like M_k and M of [8] our matrices satisfy the following theorems which can be proved

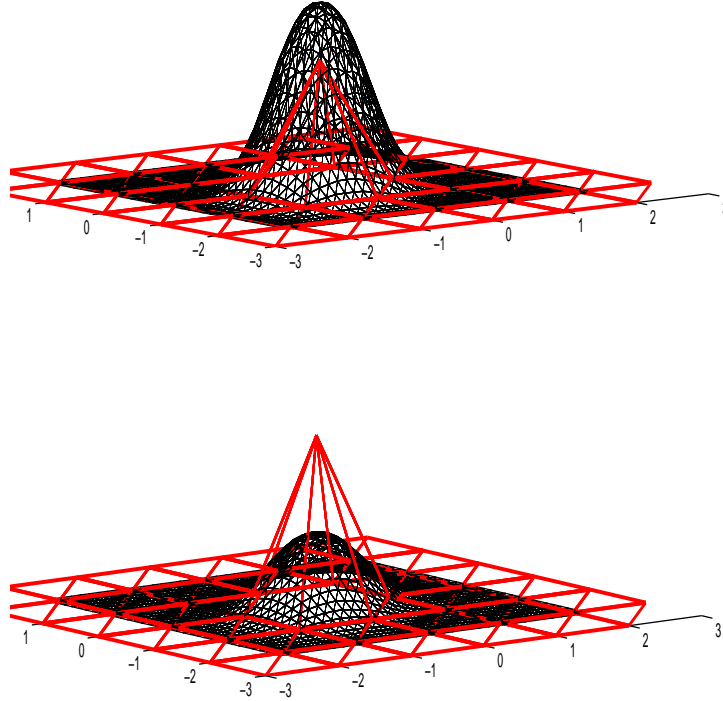


Figure 6: Non-normalized Trigonometric Box Spline Y_3 (top) does not lie in the convex hull of Initial control mesh Y_0 . Normalized Trigonometric Box Spline $\cos^2 h Y_3$ (bottom) lies in the convex hull of Y_0 . Here we have taken $h = 1$.

identically as in [8].

For a 7×1 column vector x the norm of x is defined as

$$\|x\| = \max_{1 \leq k \leq 7} |x_k|.$$

Theorem 4.1. *The stationary matrix M satisfies the following:*

- $\|Mx\| \leq \|x\|$,
- $\|M^k x\| \leq \|x\|$ for all positive integer k .

Theorem 4.2. *The non-stationary matrices $M_k, k \in \mathbb{N}$ satisfy the following:*

- $\|M_k x\| \leq \frac{\cos^2(h/2^k)}{\cos^2(h/2^{k-1})} \|x\|,$
- $\|M^{(k)} x\| \leq \frac{1}{\cos^2(h)} \|x\|.$

Theorem 4.3. $\|S_k\| \leq \frac{C(h)}{4^k} \|x\|, \forall k.$

Below, we show that our subdivision scheme converges.

Theorem 4.4. *The sequence of control meshes $\{Y_k\}$ converges to a limit surface and the limit surface is continuous.*

Proof. We consider a 7×3 column vector \mathbf{x} and study the convergence of the sequence $\{M^{(k)} \mathbf{x}\}$. Without loss of generality, we study the convergence of $\{M^{(k)} x\}$, where x is a 7×1 column vector.

Note that

$$\begin{aligned} \|(M^{(k+1)} - M^{k+1})x\| &= \|(M_{k+1}M^{(k)} - MM^k)x\| \\ &= \|((M + S_{k+1})M^{(k)} - MM^k)x\| \\ &= \|(MM^{(k)} - MM^k + S_{k+1}M^{(k)})x\|. \end{aligned}$$

By triangle inequality, this implies

$$\|(M^{(k+1)} - M^{k+1})x\| \leq \|M(M^{(k)} - M^k)x\| + \|S_{k+1}M^{(k)}x\|. \tag{4.1}$$

By Theorem 4.1 to Theorem 4.3, the above equation implies

$$(4.2) \quad \|(M^{(k+1)} - M^{k+1})x\| \leq \|M(M^{(k)} - M^k)x\| + \frac{C(h)}{4^{k+1}} \|x\|.$$

Let $\epsilon_k = \|(M^{(k)} - M^k)x\|$. Then by (4.2)

$$\epsilon_{k+1} \leq \epsilon_k + \frac{C(h)}{4^{k+1}} \|x\|,$$

which implies

$$(4.3) \quad |\varepsilon_{k+1} - \varepsilon_k| \leq \frac{C(h)}{4^{k+1}} \|x\|.$$

Now, for $m \geq k+1$

$$\begin{aligned} \|\varepsilon_m - \varepsilon_k\| &\leq \|\varepsilon_m - \varepsilon_{m-1}\| + \|\varepsilon_{m-1} - \varepsilon_{m-2}\| + \dots + \|\varepsilon_{k+1} - \varepsilon_k\| \\ &\leq C(h)\|x\| \left(\frac{1}{4^m} + \frac{1}{4^{m+1}} + \dots + \frac{1}{4^{k+1}} \right) \\ &= C(h)\|x\| \left(\frac{1}{4^{m-k-1}} + \frac{1}{4^{m-k-2}} + \dots + \frac{1}{4} + 1 \right) \frac{1}{4^{k+1}} \\ &= \frac{C(h)\|x\|}{4^{k+1}} \frac{1}{1 - \frac{1}{4}} \\ &= C(h)\|x\| \frac{1}{3 \cdot 4^k}. \end{aligned}$$

For given $\varepsilon > 0$, we can find N such that $\frac{1}{4^k} < \varepsilon$, for every $k > N$. Therefore,

$$|\varepsilon_m - \varepsilon_k| \leq \frac{C(h)}{3} \|x\| \varepsilon, \text{ whenever } m, k > N. \quad (4.4)$$

This implies the sequence $\{\varepsilon_k\}$ is Cauchy in \mathbb{R} and hence converges.

Let $\varepsilon_k \rightarrow e$. Then $\varepsilon_k = e + o(1)$. This implies

$$\|(M^{(k)} - M^k)x\| = e + o(1).$$

Therefore,

$$(M^{(k)}\mathbf{x} - M^k\mathbf{x}) \rightarrow \mathbf{E} + \Theta(1),$$

where \mathbf{E} is a fixed 7×3 matrix and $\Theta(1) \rightarrow 0$. Since $\{M^k\mathbf{x}\}$ converges, say to \mathbf{Y} , we have

$$M^{(k)}\mathbf{x} \rightarrow \mathbf{Y} + \mathbf{E} + \mathbf{O}(1).$$

This proves the convergence of $\{M^{(k)}Y_0\}$. □

The surface \mathbf{Y} is the limit surface of stationary subdivision scheme which lies in the convex hull of Y_0 .

The surface $\mathbf{Y} + \mathbf{E}$ [See Figure 5(top)] is the limit surface of non-stationary subdivision scheme which

does not lie in the convex hull of Y_0 [See Figure 6(top)]. It is observed (Theorem 4.2) that $\|M^{(k)}x\| \leq \frac{1}{\cos^2(h)}\|x\|$. Thus, $\cos^2(h)(\mathbf{Y} + \mathbf{E})$ lies in the convex hull of Y_0 [See Figure 6(bottom)] as explained in section 3.

Subdivision Matrix : We can also verify the convergence of our subdivision scheme by analyzing the subdivision matrix. Since the eigensystem of the subdivision matrix play a very important role in the convergence analysis (cf. [16, 17]), we first study the eigensystem of the subdivision matrix. More explicitly our subdivision matrix M_{k+1} , $k = 0, 1, 2, \dots$ (ref. 3.1) can be written in a more compact form:

$$M_{k+1} := \begin{bmatrix} a & \mathbf{B} \\ \mathbf{B}' & \mathbf{A} \end{bmatrix},$$

where $a = w_0(k)$,

$$\mathbf{B} = \begin{bmatrix} w_1(k) & w_1(k) & w_1(k) & w_1(k) & w_1(k) & w_1(k) \end{bmatrix},$$

$$\mathbf{B}' = \begin{bmatrix} w_2(k) & w_2(k) & w_2(k) & w_2(k) & w_2(k) & w_2(k) \end{bmatrix}^T,$$

$$\text{and } \mathbf{A} = \begin{bmatrix} w_2(k) & w_3(k) & 0 & 0 & 0 & w_3(k) \\ w_3(k) & w_2(k) & w_3(k) & 0 & 0 & 0 \\ 0 & w_3(k) & w_2(k) & w_3(k) & 0 & 0 \\ 0 & 0 & w_3(k) & w_2(k) & w_3(k) & 0 \\ 0 & 0 & 0 & w_3(k) & w_2(k) & w_3(k) \\ w_3(k) & 0 & 0 & 0 & w_3(k) & w_2(k) \end{bmatrix}_{6 \times 6},$$

which is a circulant matrix of order 6×6 . Let the eigenvalues and their corresponding eigenvectors of M_{k+1} be denoted by $\{\lambda_i, \mu_i\}$ for $i = 1, 2, \dots, 6$. Then, by direct evaluation using Mathematica 9.0, we get:

$$\lambda_1 = 1,$$

$$\lambda_2 = \lambda_3 = \frac{1}{2},$$

$$\lambda_4 = \lambda_5 = -\frac{5+6\cos h+3\cos 2h}{48\cos^4(h/2)},$$

$$\lambda_6 = \lambda_7 = \frac{1+\cos h+\cos 2h}{16\cos^4(h/2)}.$$

The corresponding eigenvectors are

$$\mu_1 = (1, 1, 1, 1, 1, 1)^T,$$

$$\mu_2 = (0, 1, 0, -1, -1, 0, 1)^T,$$

$$\mu_3 = (0, -1, -1, 0, 1, 1, 0)^T,$$

$$\mu_4 = (0, -1, 0, 1, -1, 0, 1)^T,$$

$$\mu_5 = (0, -1, 1, 0, -1, 1, 0)^T,$$

$$\mu_6 = \left(\frac{-2(2+3\cosh)}{7+9\cosh+3\cos 2h}, 0, 1, 0, 1, 0, 1 \right)^T,$$

$$\text{and } \mu_7 = \left(\frac{-2(2+3\cosh)}{7+9\cosh+3\cos 2h}, 1, 0, 1, 0, 1, 0 \right)^T.$$

So we get following eigenproperties.

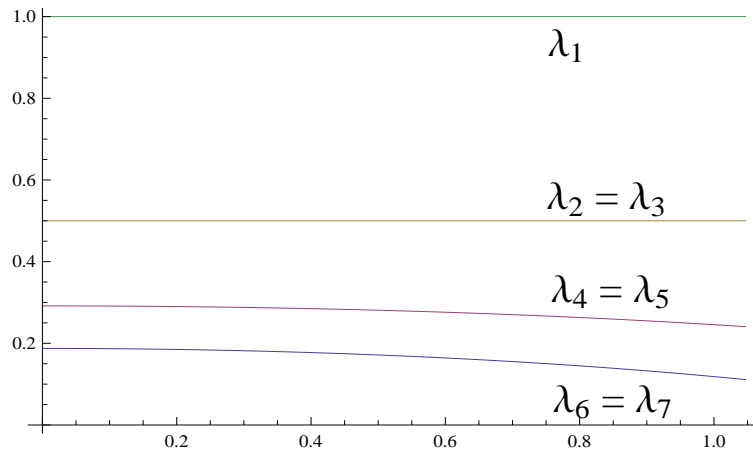


Figure 7: Figure showing the graph of eigenvalues sorted in decreasing order(top to bottom) for $0 < h < \frac{\pi}{3}$.

1. $\lambda_1 = 1, \mu_1 = (1, 1, 1, 1, 1, 1, 1)^T,$

$$|\lambda_i| < 1, \quad i = 2, \dots, 6.$$

2. $\lambda_2 = \lambda_3 > 0, |\lambda_i| < \lambda_2, \forall i > 3.$

3. $\lambda_4 = \lambda_5 \geq \lambda_6 > 0,$ and $\lambda_6 = \lambda_7.$

4. $|\lambda_4| < 0.3,$ and

$$|\lambda_6| < 0.2, \text{ for } 0 < h < \frac{\pi}{3}.$$

Since the subdivision matrix M_{k+1} satisfies the first property (see property 1), our subdivision algorithm converges by the following theorem.

Theorem 4.5. *(Convergence of a Subdivision Algorithm)(cf. [16]) Let A be a subdivision algorithm and let its eigenvalues be sorted by modulus. If $1 = \lambda_1 > |\lambda_2|$, then A converges.*

Moreover, our subdivision scheme is uniformly continuous and C^1 by the following theorem.

Theorem 4.6. *If the local subdivision matrix A satisfies the first property(ref. property 1), then the limit surface is uniformly continuous and C^1 ([16](Theorem 5.3 and Theorem 5.4)).*

5 Conclusion

A new non-stationary subdivision scheme on type-I triangulation has been derived using the non-stationary subdivision scheme that has been defined in [8]. The limit surface of this subdivision scheme is called trigonometric box-spline surface. We have also studied the convergence of the proposed scheme. This subdivision scheme is simple, effective and can be applied to geometric modeling and to construct wavelet.

Acknowledgement. This research is supported by "Innovation in Science Pursuit for Inspired Research (INSPIRE)" Fellowship of Department of Science and Technology, India bearing the Regd. No. DST/INSPIRE Fellowship/2016/IF160366. So the authors are grateful to Department of Science and Technology, India.

References

1. Boor C. de, Hollig K., Riemenschneider S., Box Splines, *Springer-Verlag* (1993).

2. Catmull E., Clark J., Recursively generated B-Spline surfaces on arbitrary topological meshes, *Computer Aided Design*, **10** (1978), 350-355.
3. Conti C., Donatelli M., Novara P., Romani L., A linear algebra approach to the analysis of non-stationary subdivision for 2-manifold meshes with arbitrary topology, *arXiv:1707.01954v1[math.NA]* (2017).
4. Doo D., Sabin M., Behaviour of recursively division surfaces near extraordinary points, *Computer Aided Design*, **10** (1978), 356-360.
5. Dyn N., Gregory J. A. and Levin D., A 4-Point interpolatory subdivision scheme for curve design, *Compt. Aided Geom. Design*, **4** (1987) 257-268.
6. Dyn N., Gregory J. A. and Levin D., Analysis of uniform binary subdivision scheme for curve design, *TR/09, Dept. of Maths. and Stats, Brunel University, Britain* (1991).
7. Jena M. K., Shunmugaraj. P, Das P.C., A subdivision algorithm for trigonometric spline curves, *Compt. Aided Geom. Design*, **19** (2002), 71-88.
8. Jena M. K., Shunmugaraj. P, Das P.C., A non-stationary subdivision scheme for generalizing trigonometric spline surfaces to arbitrary meshes, *Compt. Aided Geom. Design*, **20**, (2003) 61-77.
9. Koch P. E., Multivariate trigonometric B-splines, *J. Approx. Theory*, **54** (1988), 162-168.
10. Koch P.E., Lyche T., Neamtu M., Schumaker L., Control curves and knot insertion for trigonometric splines, *Adv. Comput. Math.*, **3** (1995), 405-424.
11. Lai M. J., Schumaker L. L., Spline Functions on Triangulations, *Cambridge university press, Cambridge*, (2007).
12. Lyche T., Winther R., A stable recurrence relation for trigonometric B-splines, *J. Approx. Theory*, **25** (1979), 266-279.

13. Lyche T., Schumaker L. L., Stanley S., Quasi interpolation based on trigonometric splines, *J. Approx. Theory*, **95** (1998), 280-309.
14. Morin G., Warren J., Weimer H., A subdivision scheme for surface revolution, *Compt. Aided Geom. Design*, **18** (2001), 483-502.
15. Peters J., Reif U., Subdivision Surfaces, *Springer*, (2008).
16. Qu R., Recursive subdivision algorithms for curve and surface design, Ph. D Thesis, Department of Mathematics and Statistics, Brunel University, Britain(August 1990).
17. Qu R., Agarwal R. P., Smooth Surface Interpolation to Scattered Data Using Interpolatory Subdivision Algorithms, *Computers Math. Applic.*, **32** (1996), 93-110.
18. Reif U., A unified approach to subdivision algorithms near extraordinary vertices, *Compt. Aided Geom. Design*, **12** (1995), 153-174.
19. Rogers D. F., An Introduction to NURBS: With Historical Perspective, *Morgan Kaufmann*, (2001).
20. Schoenberg I. J., On trigonometric spline interpolation, *J. Math. Mech.* **13(5)** (1964), 795-825.
21. Schumaker L.L., Spline Functions: Basic Theory, third ed., *Cambridge University Press*, (2007).
22. Schumaker L. L., Trass C., Fitting scattered data on spherelike surfaces using tensor products of trigonometric and polynomial splines, *Numer. Math.*, **60** (1991) 133-144.

